MEMS with $\Sigma - \Delta$ Type of Feedback Loop Control as an Iterative Map

Mathieu Pladys
Département de Génie Electrique et Informatique
Institut National des Sciences Appliquées de Toulouse
Toulouse, France

Elena Blokhina
School of Electrical, Electronic and Mechanical Engineering
University College Dublin
Dublin, Ireland

***Abstract*— In this work, we consider a system that consists of a microresonator and a $\Sigma\,\Delta$ type feedback loop control which is typically a part of inertial sensors. We describe this architecture as a dynamical system (an iterative difference equation) in the time domain in order to study possible periodic solutions in the output.**

I. Introduction

Closed loop microelectromechanical (MEMS) architectures which include a physical sensing element and a $\Sigma\Delta$ modulator structure to serve as a feedback loop for the sensor (fig. 1) have been proposed, designed and implemented in the recent years as an effective part of inertial sensors [1]–[5]. The main idea behind this topology is that the displacement of the proof mass, which depends on the input, is maintained around its equilibrium due to the feedback force and the applied input is represented as an average at the output of the comparator. On top of many advantages of this architecture, closed loop sensors which incorporate the analogue to digital conversion within the loop, produce a digital signal in the output.

For this type of systems, it has been shown that periodic sequences (cycles) appear at the output of the comparator [6]–[9]. These cycles may be utilised for self-calibration purposes in the system without input since the MEMS parameters may be extracted from their characteristics [8].

Our aim in this paper to propose a simple model in the form of a map (discrete-time system) in order to study this architecture as a *dynamical system*. This approach gives a glance at the behaviour of the system from the standpoint of nonlinear dynamics and allows us not only to qualitatively explain the appearance of periodic cycles of the map, but also to study the behaviour of the system over a wide range of control parameters. In particular, we introduce the plane spanned by parameters of the system where we define regions of admissibility of cycles. We also outline similarities which arise between conventional $\Sigma\Delta$ [10] modulation and another MEMS topology — pulsed digital oscillators (PDO) [11] — which also utilises a $\Sigma\Delta$-like feedback and combines it with pulsed actuation.

II. Statement of the Problem

The displacement of the mechanical resonator from fig. 1 as a function of time $\xi(t)$ is described by the well-known mass-spring-damper equation:

$$m\ddot{\xi}(t) + b\dot{\xi}(t) + k\xi(t) = F(t) \tag{1}$$

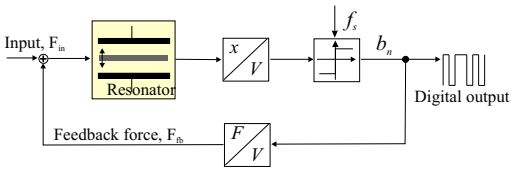

Fig. 1. Block diagram of the MEMS Sigma-Delta architecture.

where m is the mass of the plate, b is the damping factor and k is the effective spring constant. The net force $F(t)$ consists from the feedback $F_{fb}(t)$ and the input $F_{in}(t)$. Here we assume that the feedback actuation takes place through electrostatic force which is the case for many systems. For eq. (1), $F_{fb}(t)$ is written in the following form:

$$F_{fb}(t) = \begin{cases} -\varepsilon_0 A V_0^2 / \left(2[g+\xi(t)]^2\right) & \text{if} \quad \xi(t) \geq 0\,, \\ +\varepsilon_0 A V_0^2 / \left(2[g-\xi(t)]^2\right) & \text{if} \quad \xi(t) < 0\,, \end{cases} \tag{2}$$

where ε_0 is the vacuum permittivity, A is the electrode area and V_0 is the control voltage.

The nature of the electrostatic force is nonlinear, though it is usual to linearise it by dropping off the small displacement $\xi(t)$ compared to the equilibrium gap g. As an alternative, expanding the nonlinear part of the electrostatic force, one can use the following representation for linearised $F_{fb,lin}(t)$:

$$F_{fb,lin}(t) \approx -\mathrm{sgn}(\xi) F_0 + 2F_0\xi/g \tag{3}$$

which, substituted in (1), produces a shift in the natural frequency $\omega = \sqrt{k/m}$. Thus, the new frequency now is $\omega_0 = 2\pi f_0 = \omega\sqrt{1 - 2F_0/g\omega^2}$ where $F_0 = \varepsilon_0 A V_0^2/2g^2$. The linearised feedback force, therefore, can be simply written as $F_{fb,lin}(t) = -\mathrm{sgn}(\xi(t))F_0\,.$

Let us introduce the following variables: time $\tau = \omega_0 t$, displacement $x = m\omega_0^2\xi/F_0$, dissipation $\beta = b/(2m\omega_0)$ and normalised input $a = F_{in}/F_0$. We will consider in this paper that a is a constant. Indeed, since the natural and sampling frequencies are high, we may assume a time-varying input to be constant over relatively large sampling events.

Thus, we obtain the following normalised equation instead of (1):

$$\ddot{x} + 2\beta\dot{x} + x = a - \mathrm{sgn}(x)\,, \tag{4}$$

where now $\dot{x}$ represents the derivative with respect to dimensionless time τ.

The solution of a mass spring damper equation with the left part as in (4) and, in the most general case, with some $F(t)$ in the right part consists of two terms, namely, the decaying free oscillations $x_1(t)$ and the forced ones $x_2(t)$. While the expression for $x_1(\tau)$ is well known, we note that for arbitrary $F(t)$ the forced oscillations may be found as follows:

$$x_2(\tau) = \int_0^\tau \frac{F(t)e^{-\beta(\tau-t)}}{\sqrt{1-\beta^2}} \sin(\sqrt{1-\beta^2}(\tau-t))dt\,, \qquad (5)$$

where the integral can be easily solved in the interval $[0,\tau]$ for certain functions $F(t)$, for instance, if it is a constant F_0. Thus, solving (5) for $F(t) = F_0$ and introducing the new variable $y = -(\beta x/\sqrt{1-\beta^2}) - v/\sqrt{1-\beta^2}$ (where $v = \dot{x}$ is the velocity), one obtains

$$\begin{aligned}
x_1(\tau) =& e^{-\beta\tau}\left(x_0\cos(\sqrt{1-\beta^2}\tau) - y_0\sin(\sqrt{1-\beta^2}\tau)\right)\,,\\
y_1(\tau) =& e^{-\beta\tau}\left(y_0\cos(\sqrt{1-\beta^2}\tau) + x_0\sin(\sqrt{1-\beta^2}\tau)\right)\,,\\
x_2(\tau) =& F_0 - F_0\, e^{-\beta\tau}\cos(\sqrt{1-\beta^2}\tau) -\\
& \frac{F_0\,\beta e^{-\beta\tau}}{\sqrt{1-\beta^2}}\sin(\sqrt{1-\beta^2}\tau) = F_0\,\zeta(\beta,\tau)\,,\\
y_2(\tau) =& -\frac{F_0\,\beta}{\sqrt{1-\beta^2}} + \frac{F_0\,\beta e^{-\beta\tau}}{\sqrt{1-\beta^2}}\cos(\sqrt{1-\beta^2}\tau) -\\
& F_0\, e^{-\beta\tau}\sin(\sqrt{1-\beta^2}\tau) = F_0\,\eta(\beta,\tau)\,.
\end{aligned} \qquad (6)$$

Knowing the solutions, it is easy now to obtain an iterative map from (6) by simply substituting x_n and y_n instead of the initial conditions x_0 and y_0, the dimensionless sampling time $\tau_s = \omega_0 T_s$ instead of τ and $F_n = a - \mathrm{sgn}(x_n)$ instead of F_0 (F_n is constant during one sampling event). Thus, the sampled system is described now by the following equations:

$$\begin{pmatrix} x_{n+1} \\ y_{n+1} \end{pmatrix} = \alpha\mathbf{R}(2\pi\, f\sqrt{1-\beta^2}) \begin{pmatrix} x_n \\ y_n \end{pmatrix} + F_n \begin{pmatrix} \zeta(\beta,f) \\ \eta(\beta,f) \end{pmatrix}, \qquad (7)$$

where we introduce the parameters $\alpha = \exp(-\beta\tau_s) = \exp(-2\pi\beta f)$ (or, returning to the original variables, $\alpha = \exp[-bT_s/(2m)]$) and the normalised frequency $f = \tau_s/(2\pi)$ ($f = f_0/f_s$). We also used the notation $\mathbf{R}(\alpha)$ in (7) to denote the rotation matrix. The terms ζ and η caused by the presence of $F(t)$ in the right part of equation (4) are functions of the parameters α, f and τ_s and not of x_n and y_n. The term F_n in (7) can be generalised as

$$F_n = a - \mathrm{sgn}(x_{n-D}) \qquad (8)$$

where $D \geq 0$ denotes a possible delay in the architecture shown in fig. 1. The system (7) is a piecewise-smooth discontinuous map. Piecewise-smooth maps model many physicals systems, including switching circuits and systems with oscillatory behavior [12], [13].

Strictly speaking, (7) is written for the *underdamped* case when $\beta < 1$. For the *overdamped* case, $\beta > 1$, the expression in the root $\sqrt{1-\beta^2}$ becomes negative and f itself complex. The map (7) can still be written in its form if, considering that the expression $2\pi f$ is now complex, we recall that $\cos(ix) = \cosh(x)$ and $\sin(ix) = i\sinh(x)$ in the rotation matrix. Since the root $\sqrt{1-\beta^2}$ was also used in the definition of y, the second variable must be transformed $y^* \to -iy$. (After these changes, all variables and parameters in (7) will be still real).

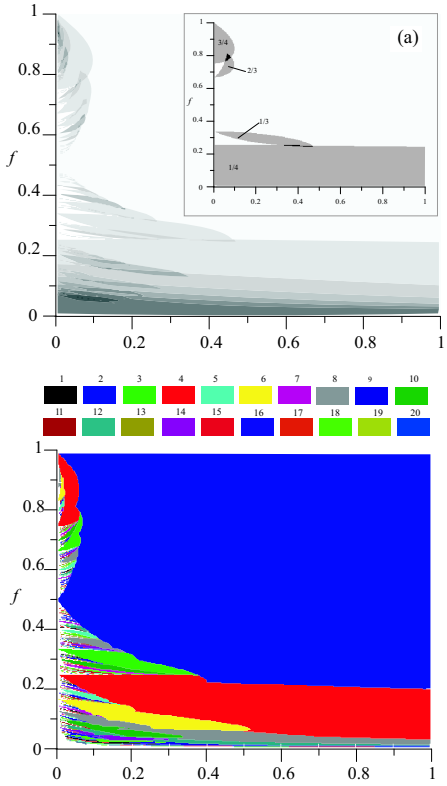

Fig. 2. Underdamped case. (a) Regions of admissibility (with overlapping) for N-cycles with $1 \leq N \leq 20$ in the parameter plane calculated from (10). The insert of the figure shows the form of the tongues that correspond to odd (by the example of the 3-cycle) and even (by the example of 4-cycle) cycles. (b) Parameter plane with tongues that correspond to different cycles obtained from numerical simulations of the map (7) with the zero initial conditions.

We note that in the map (7), the first term $\alpha\mathbf{R}(2\pi f\sqrt{1-\beta^2})$ represents the decaying eigen oscillations of the resonator (with the parameter α responsible for decay). The second term which contains ζ and η represents the response of the oscillator to a square pulse with constant amplitude.

The form of the map (7) resembles the map proposed for the pulsed digital oscillator topology [11]. Due to the difference in driving of the PDO and the studied system, the iterative map for the PDO is a particular case of the map (7) with $\zeta = 0$ and $\eta = \text{const}$ studied in details in refs. [11], [14], [15].

III. Periodic solutions

It is well known that the conventional $\Sigma - \Delta$ architecture displays periodic sequences (cycles) in the output [10]. A microresonator embedded into this type of structure displays periodic behaviour as well [8]. In this section we study periodic sequences $\{(x_n, y_n)\}$ that are produced by the map (7).

Assume that there is a N-periodic sequence of signs b_n which is defined as

$$b_n = \mathrm{sgn}(x_n). \qquad (9)$$

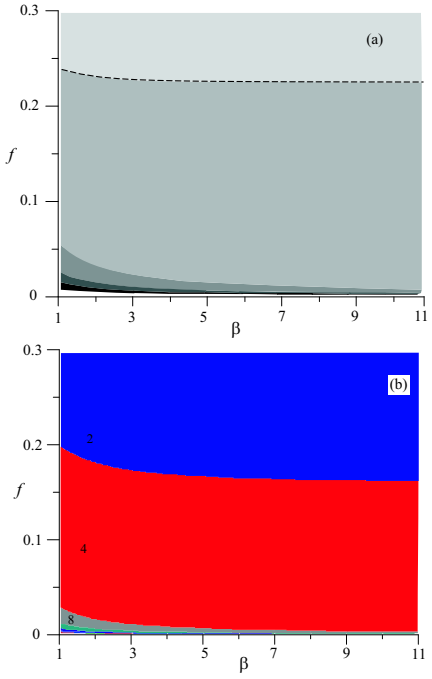

Fig. 3. Overdamped case. (a) Regions of admissibility (with overlapping) for the 2, 4, 8, 12, 16 and 24-cycles. (b) Parameter plane with tongues that correspond to different cycles obtained from numerical simulations of the map (7) with the zero initial conditions.

Under the condition $x_n = x_{n+N}$, the following sequence determines the N-cycle:

$$\begin{pmatrix} x_n \\ y_n \end{pmatrix} = \mathbf{A}(N\psi) \sum_{j=1}^{N} \alpha^{N-j} R((N-j)\psi) F_{n+j-1} \begin{pmatrix} \zeta \\ \eta \end{pmatrix} . \tag{10}$$

In (10), A is the following matrix

$$\mathbf{A}(N\psi) = \left(\mathbf{I} - \alpha^N \mathbf{R}(N\psi)\right)^{-1} , \tag{11}$$

$\mathbf{I}$ is the identity matrix, $\psi = 2\pi f\sqrt{1-\beta^2}$ and F_n depends on x_n according to (8).

A cycle given by (10) will be asymptotically stable. Indeed, let us consider the evolution of a small disturbance of some point x_n, y_n that belongs to the N-cycle. Let also this disturbance lies in the δ-neighbourhood of this point such that $\delta = \min|x_n| > 0$ for all N. In this case, evolution after k iterations of $\tilde{x}_n = x_n + \delta x$ and $\tilde{y_n} = y_n + \delta y$ is defined as

$$\begin{pmatrix} \tilde{x}_{n+k} \\ \tilde{y}_{n+k} \end{pmatrix} = \begin{pmatrix} x_{n+k} \\ y_{n+k} \end{pmatrix} + \alpha^k \mathbf{R}(k\psi) \begin{pmatrix} \delta x \\ \delta y \end{pmatrix} . \tag{12}$$

As is seen from this formula, the disturbed trajectory approaches the initial one since $\alpha < 1$.

Thus, the strategy is the following:

- Assume the sequence b_n for the sign of the position;
- For fixed β, f and a, calculate (x_n, y_n) in (10);
- Check if the condition (9) is fulfilled.

Varying β and f over wider regions with implementation of the above strategy allows one to obtain the parameter plane (β, f) with regions of cycles admissibility — so called tongues.

IV. System with no input

First we consider the system with no input, i.e. $a = 0$. The reasons of this study are: a) for certain types of inertial sensors, resonant accelerometers, a proof mass changes the strain of an attached resonator, hence changing its resonant frequency. The scheme may also be used as a part of a self-sustained oscillations system [5]. The parameter of interest in this case is the change of the frequency, and in terms of the model (7) we have only two parameters that entirely control the dynamics of the system — β and f; b) for the topology with no input displays periodic sequences (cycles) at comparator's output which may be used for self-testing purposes.

For a linear resonator, the output waveform in this case will be a sinusoid, and, therefore, one can obtain the sequence b_n for the expression (10) as the sign of a sampled sinusoid:

$$b_n = \mathrm{sgn}(\cos(2\pi k M/N + \varphi_0)) \tag{13}$$

where φ_0 is an arbitrary phase and $1 \le k \le N$. The ratio M/N defines the rotation number of a cycle, i.e. the number of loops around the origin a trajectory makes in one iteration. The expression (13) is valid not only for the case of high-Q resonators but also for cycles in the overdamped case (with no input for the both cases). The most general discussion on admissible sequences is given in [9].

The parameter plane (β, f) for tongues with rotation numbers M/N, $0 < N < 15$ is shown in fig. 2 (for the underdamped case) and fig. 3 (for the overdamped case). The grey areas show possible values of parameters at which a specific cycle can be observed in the system. As is seen from the figure, the tongues overlap (shown by darker gray shades): at the same β and f there coexist several cycles and which one of them will eventually be displayed by the system depends only on initial conditions. For example, the planes of parameters calculated for the zero initial conditions are shown in fig. 2(b) and 3(b). For the areas of tongues overlapping, one can plot basins of attraction, i.e. the areas on the plane spanned by the initial conditions x_0 and y_0 (fig. 4(c)). In general, the picture that one observes for the underdamped case is very similar to the PDO dynamics [14], [15] in the sense that tongues and overlapping areas are very typical for the system.

As far as the tongues defined by (10) are concerned, firstly we note that the 2-cycle (the area shown in blue) can formally exist everywhere in the plane (it is shown by the lightest grey shade in figs. 2(a) and 3(a)). In practice, for certain parameters it would be almost impossible to obtain it since the initial conditions demanded for it may be unrealsitic. We also note that only even cycles exist for the overdamped resonator.

Secondly, we draw the attention to the different forms of tongues that correspond to odd and even N for the underdamped case (see the insert in fig. 2(a) where the tongues with $N = 3$ and $N = 4$ are shown). Though the odd tongues have conventional form, the even tongues are rather unusual and "cut off " large areas in the plane. To prove it, we obtained explicit form for the 3- and 4-cycles directly from (10) (which we do not give here due to its complex form).

The points x_n as functions of the parameter f at a fixed β for the 3- and 4-cycles are shown in fig 4(a) and (b) respectively. Since $\mathrm{sgn}(x_n)$ must be the same as the sequence

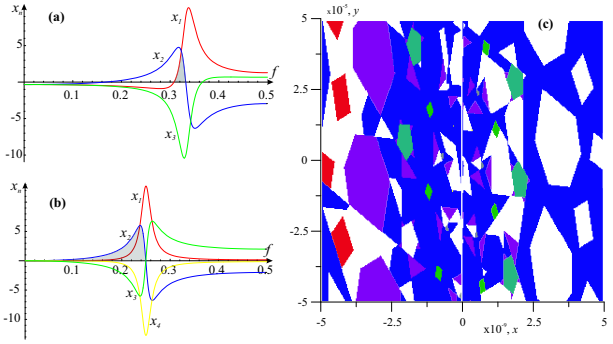

Fig. 4. Basins of attraction of different cycles: at the same values of parameters various output is possible depending on initial conditions.

b_n which generated the cycle, we highlight the interval of the f axis over which these cycles are admissible and this area is precisely the cross-section of the tongues from the plane 2(a).

V. System with input

In this section, we briefly discuss results for the topology which is used with an input. Here, we present results only for the overdamped case, though the topology may be used also with high-Q resonators [3]. We also restrict ourselves to the case when the sampling frequency is much higher than the natural frequency of the resonator and the input a is constant.

As noted before, the system output represents a cycles with a frequency that depends on the input and on the parameters of the device. Since this topology is based on the same ideas as a $\Sigma\Delta$ modulator, the input is obtained as an average of the output cycle. First we note that the average output x_{out} (over a cycle) as a function of the input a is close to a linear dependance, but a magnified part of the plot reveals that it consists of a number of steps (fig. 5). We recall that the same situation is observed in a conventional $\Sigma\Delta$ modulator [10] and in the PDO [11], [14]. Such steps appear due to frequency locking and indicate that particular cycles exist in a finite interval of a control parameter.

The output of the system can be presented in the plane of parameters (β, a), see fig. 6(a) (similar to fig. 2 and 3). To plot this plane, we choose those sequences b_n for the formula (10) that correspond to the widest steps in figure 5. Now, the steps in $x_{out}(a)$ can be considered as cross-sections of areas in which cycles are admissible. As is seen from the plane 6, width of steps depends on the dissipation β: the higher

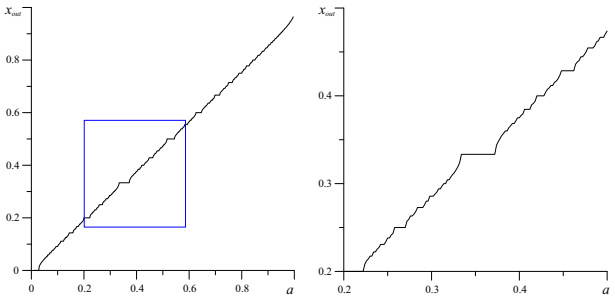

Fig. 5. Average output as a function of the input a and the magnified part of the plot.

the dissipation, the smaller the width (and, consequently, the higher the resolution of the system). Figure 6(b) shows the average output coded by different colours: from 0 (blue) to 1 (red).

VI. Conclusion

An iterative equation was derived to describe a microresonator whose oscillations are sustained by a $\Sigma\Delta$ type feedback loop in the time domain. For this system, periodic behaviour is a subject of interest, and the proposed model allows one to explain and find the conditions of periodic sequences (cycles) at the output of the system. The technique we used gives a representation of the behaviour of the system over wide ranges of the control parameters. In particular, the study has shown how the areas of admissability of cycles change with variation of dissipation and the sampling frequency.

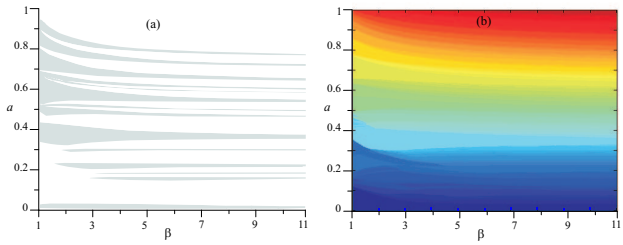

Fig. 6. (a) Tongues that correspond to the widest steps of the plot 5 in the (a, β) plane. (b) The average output for different normalised inputs a and dissipations β presented by different colours: from 0 (blue) to 1 (red)

References

[1] B. E. Boser and R. T. Howe, "Surface micromachined accelerometers," *IEEE Trans. Syst. Sci. Cybernetics*, vol. 31, p. 366, 1996.

[2] M. Kraft, C. P. Lewis, and T. Hesketh, "Closed loop silicon accelerometers," *IEE Proc. – Circuits, Devices Syst.*, vol. 145, p. 325, 1998.

[3] J. Wu and L. R. Carley, "Electromechanical $\Delta\Sigma$ modulation with high-Q micromechanical accelerometers and pulse density modulated force feedback," *IEEE Trans. Circuits Syst. I*, vol. 53, p. 274, 2006.

[4] J. Soen, A. Voda, and C. Condemine, "Controller design for a closed-loop micromachined accelerometer," *Control Engineering Practice*, vol. 15, p. 57, 2007.

[5] C. Comi, A. Corigliano, G. Langfelder, and et al, "A resonant microaccelerometer with high sensitivity operating in an oscillating circuit," *J. Microelectromech. Syst.*, vol. 10, p. 1140, 2010.

[6] G. K. Fedder, "Simulation of microelectromechanical systems," Ph.D. dissertation, U. C. Berkeley, 1994.

[7] M. Kraft, "Closed loop accelerometer employing oversampling conversion." Ph.D. dissertation, Coventry University, 1997.

[8] E. Colinet, J. Juillard, L. Nicu, and C. Bergaud, "Digital self-calibration method for MEMS sensors," *IEEE Trans. Instrum. Meas.*, vol. 54, p. 1438, 2005.

[9] J. Juillard and E. Colinet, "Using Tsypkins approach for the study of a class of mixed-signal nonlinear systems," *IEEE Trans. Circuits Syst. I*, vol. 53, p. 2746, 2006.

[10] O. Feely and L. Chua, "The effect of integrator leak in Σ–Δ modulation," *IEEE Trans. Circuits Syst.*, vol. 38, p. 1293, 1991.

[11] M. Domínguez, J. Pons-Nin, J. Ricart, A. Bermejo, E. Figueras Costa, and M. Morata, "Analysis of the $\Sigma - \Delta$ pulsed digital oscillator for MEMS," *IEEE Trans. Circuits Syst. I*, vol. 52, p. 2286, Nov. 2005.

[12] V. Avrutin, M. Schanz, and S. Banerjee, "Multi-parametric bifurcations in a piecewiselinear discontinuous map," *Nonlinearity*, vol. 19, 2006.

[13] D. J. W. Simpson and J. D. Meiss, "Neimarksacker bifurcations in planar, piecewise-smooth, continuous maps," *J. Appl. Dyn. Syst.*, vol. 7, 2008.

[14] A. Teplinsky and O. Feely, "Limit cycles in a MEMS oscillator," *IEEE Trans. Circuits Syst. II*, vol. 55, p. 882, Sept. 2008.

[15] E. Blokhina, O. Feely, and M. Dominguez, "Dynamics of the MEMS pulsed digital oscillator with multiple delays in the feedback loop," in *Proc. of IEEE ISCAS 2009*, Taipei, Taiwan, 24–27 May 2009, p. 1903.